Stanford Exploration Project, Report 123, October 31, 2005, pages 57–69

Direct migration: The only way

Brad Artman[1]

ABSTRACT

Correlating transmission wavefields to produce reflection wavefields contains in its rigorous definition the mandate of processing data due to only a single source. If more than one source is contained in the wavefield, crosstalk between the sources will produce a data volume that is not the same as shot gathers with impulsive sources at each receiver location. When attempting to image the subsurface with the truly unknown ambient noisefield, parameterizing the field data by individual sources is impossible.

For truly passive data, the source and time axis are inextricably combined, naturally and by processing. This changes direct migration to something more akin to planewave migration. Since the direct arrival from each source can not be expected to sum together with a common time-delay, the summation manufactures a source wavefront with temporal topography rather than a planewave.

The Fourier transform of field data as a single wavefield provides insight into how sources are summed during correlation. Also, the transform simultaneously stacks away useless waiting periods between useful energy bursts and reduces the data volume. Previously, white, zero-phase source functions were invoked to avoid the summation problem. However, neither assumption is likely in the real environment of a long term experiment.

INTRODUCTION

Through one-way reciprocity, Wapenaar et al. (2004) shows how to synthesize reflection data from passively collected seismic data for 3D inhomogeneous media. Key in the proof is the distinction that correlations from only single sources may be calculated and then summed over many sources to produce the correct result. This is simple when utilizing earthquake codas (Nowack et al., 2003) or using novel experimental geometries for active surveys (Yu and Schuster, 2004). This is impossible when imaging with truly passive data where the source is the unknown ambient noisefield.

I assume that field data from a passive recording campaign can neither be parameterized by nor separated into wavefields from individual sources. In this case, correlation of the entire long data volume leads to an unavoidable summation of the wavefields from all the subsurface sources. Through Fourier analysis of correlation, I will show this inherent summation due to processing all sources as one large wavefield.

[1]**email:** brad@sep.stanford.edu

Summing the wavefields from all sources violates the rigorous definition of the result of correlating traces from a passive data collection. The output volume is not identical to the conventional reflection experiment. This report assumes the utility (Artman and Shragge, 2003) and mathematic justification (Artman et al., 2004) for direct migration of passive data as a starting point. Several synthetic models are presented to highlight the complexity introduced by not separating individual wavefields for processing as well as successful imaging with the direct migration technique. Finally, images from the passive array installed at the Valhall oil prospect in the North sea will be introduced.

WAVEFIELD SUMMATION

To calculate the Fourier transform of the reflection response of the subsurface, $R(\mathbf{x}_r, \mathbf{x}_s, \omega)$, Wapenaar et al. (2004), proves

$$2\Re[R(\mathbf{x}_r, \mathbf{x}_s, \omega)] = \delta(\mathbf{x}_s - \mathbf{x}_r) - \int_{\partial D_m} T(\mathbf{x}_r, \xi, \omega) T^*(\mathbf{x}_s, \xi, \omega)\, \mathrm{d}^2\xi \ . \tag{1}$$

The vector $\mathbf{x}$ will correspond herein to horizontal coordinates, where subscripts r and s indicate different station locations from a transmission wavefield. After correlation they acquire the meaning of receiver and source locations, respectively, associated with an active survey. The RHS represents summing correlations of windows of passive data around the occurrence of individual sources, at locations ξ, on the domain boundary ∂D_m that surrounds the subsurface region of interest. The transmission wavefields $T(\xi)$ contain only one subsurface source.

Equation 1 dictates that the correlations of transmission wavefields must only be from individual transmission wavefields recorded over an interval, t, during which a single source is actively probing the subsurface. In this case, the zero-time of the correlations are correctly shared by the output of each correlation operation since each result is zero-phase. If more than one source function is active during a time window, or it is impractical to window the raw data around individual sources, the result of correlating the raw data will not yield the reflection wavefield R.

In practice, raw data are collected over a long time and sources are weak and/or overlapping. For transmission wavefields, the time axis and the shot axis are naturally combined. If we assume that n_s individual sources, and the reflections that occur t seconds afterward, are distributed at intervals within the total recording time τ, field data can only be parameterized $T_f(\mathbf{x}_r, \tau)$. Both t and τ represent the real time axis, though I will parameterize different wavefields with them with the understanding that $\max(t)$ is the two-way time to the deepest reflector of interest and τ is the real time axis from the beginning to the end of the total recording time such that

$$\max(\tau) = \max(t) n_s + \sum_{j}^{n_s} \texttt{wait-time}_{\texttt{j}} \ . \tag{2}$$

I will further adopt the conventions ω for the frequency domain dual variable of t, and ϖ for the frequency domain dual variable of τ.

Without knowing when sources happen, and acknowledging that the `wait-time` between shots can also be negative, it is impossible to separate field data into individual wavefields when attempting to image with the ambient noisefield. In this case, equation 1 can only be implemented with a single time function of length τ

$$\tilde{R}(\mathbf{x}_r, \mathbf{x}_s, \varpi) = T_f(\mathbf{x}_r, \varpi) T_f^*(\mathbf{x}_s, \varpi). \tag{3}$$

The immediate ramification of this formulation can be considered by Fourier analysis. Correlation of more than a few hundred samples is more efficiently performed in the Fourier domain, $C(\omega) = B(\omega)A^*(\omega)$, so I will first consider the general definition of the discreet Fourier transform (DFT). The DFT of a signal $f(\tau)$ can be evaluated for a particular frequency ϖ,

$$F|_\varpi = \mathrm{DFT}[\, f(\tau)]|_\varpi = \frac{1}{\sqrt{n_\tau}} \sum_\tau f(\tau) \mathrm{e}^{-i\varpi\tau} \, . \tag{4}$$

If the long function $f(\tau)$ is broken into N short sections, $g_n(t)$, of the same length, the amplitude of a particular frequency ϖ can also be calculated

$$\mathrm{DFT}[\, f(\tau)]|_\varpi = N^{-3/2} \sum_{n=1}^{N} \mathrm{DFT}[g_n(t)]|_\omega = N^{-3/2} \mathrm{DFT}[\sum_{n=1}^{J} g_n(t)]|_\omega \tag{5}$$

by simply changing the order of summation for convenience. The only requirement for the equation above is for both of the two different length transforms to contain the particular frequency being calculated (ie. a particular frequency where $\varpi = \omega$ is possible as dictated by the Fourier sampling theorem). The longer transform has many more frequencies at a smaller sampling interval between the shared values calculated by the short transform of the stacked data.

For passive field data, $f(\tau)$ is $T_f(\tau)$, and the $g_n(t)$ are $T(\mathbf{x}_r, \xi, t)|_{\xi=n}$ as well as background noise between sources. Thus, correlating a single long recording from many sources implicitly stacks the wavefields from individual sources at each frequency. For passive data, the time axis and the shot axis are combined in nature (by sources refusing to wait in turn) and in processing (by seismologists incapable of or refusing to process individual time windows). However, this transform only supports a time signal of length t and is aliasing the long field record.

What of the intermediate frequencies ϖ that would be lost by stacking the time windows? It is necessary to remove these. Fine sampling in frequency carries information about the late time samples of the signal's dual representation. After correlation, shot records in the time domain must be windowed to remove late lag correlations which are superpositions of correlations of the different sources convolved with the earth model. These are completely uninterpretable in terms of the desired product $R(\mathbf{x}_r, \mathbf{x}_s, t)$ and will be noise in further processing. If the result needs truncation after inverse transform, it is more efficient to only transform the part of the result desired.

Time windowing has a Fourier dual operation. The Fourier sampling theorem, solved for Δt is

$$\Delta t = 1/(N \Delta f) \, .$$

Subsampling the frequency axis increases Δf by a, and reduces the number of samples to N/a. The new time domain trace length is $\Delta t\ N/a$. Removing every other frequency, $a = 2$, halves the length of the trace in the time domain. This process is the Fourier dual of reducing the Nyquist frequency by subsampling the time axis. Importantly, the ability to rearrange the order of summation in equation 5 or subsample the Fourier domain representation of signal to alias it means that the spectra of the two different length transforms are not related by smoothing. Instead, the short one is a subsampled version of the long one where all frequency samples shared by the two are identical.

The left column of Figure 1 shows a processing flow of a simple time domain signal with a zoomed in view of each trace (the first 32^{nd} of the axis) on the right. The top trace is the input signal. The middle trace is its autocorrelation. The bottom trace maintains a part of the autocorrelation result deemed important. To compute the bottom trace, the input was subsampled by 8 in the Fourier domain, multiplied by its conjugate, and inverse transformed. To facilitate plotting, the trace was padded with zeros. Identical results are obtained by time-domain stacking and Fourier domain subsampling as long as the level of decimation does not alias the acausal lags of the correlation into the positive lags.

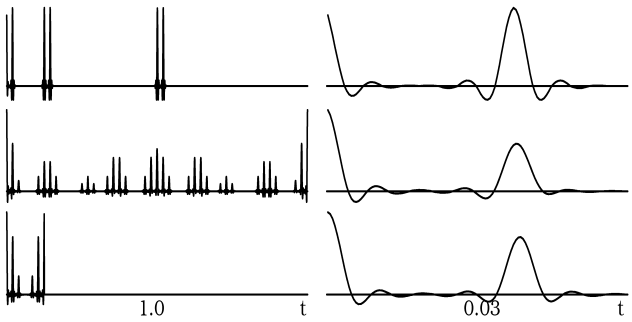

Figure 1: Right column is 32x zoom of left beginning at $t = 0$. (top) Idealized signal of three identical subsurface sources. (middle) Autocorrelation. (bottom) Autocorrelation performed with every 8^{th} frequency. Zero values are padded on the bottom trace to facilitate plotting. brad1-freq [ER]

Subsampling in one domain is not an identical operation to windowing in the dual domain. The periodicity of the Fourier transform dictates that subsampling leads to aliasing rather than true truncation. Aliasing the time domain is more efficiently performed by summing short time windows before making the correlations and thereby greatly reducing the amount of computation required. Knowing that the late time lags of correlation are aphysical for passive imaging, the above analysis shows that only the frequency samples at intervals ω, associated with records of length t, need to be inverse transformed after correlation. Since correlation is linear, we only need to calculate the frequency domain representation of the field data at this reduced sampling interval. The definition of the DFT shows that this is equivalent to first stacking the long time axis of the data. The random background and instrument noise between sources is diminished by the stacking of the time axis which also decimates a potentially enormous data volume.

Under the assumption that all the source functions recorded in the data are white and uncorrelated, the summation of the source wavefields may not be to harmful and $\tilde{R} \approx R$. Further, if the sources are all continuously ringing, and thus zero-phase over the recording, the correlations will not have residual phase. In my previous reports, both of these assumptions

were made (sometimes not intentionally), which I now believe highly improbably for a real earth experiment. To utilize bursts of local seismicity for imaging, cross-correlating traces to make shot gathers makes $\tilde{R} \neq R$. The situation is directly analogous to summing two or more shot-records. While it may be useful for some applications, this sum can not be treated as a single record with an impulsive source. Cross-talk is introduced due to the inability to separate energy from the distinct experiments.

Stacking wavefields

The time domain stacking shown in equation 5 that is implied by correlating field data with equation 3 can be explored by considering two transmission wavefields, $a(\mathbf{x}_r, t)$ and $b(\mathbf{x}_r, t)$, from individual sources. When placed randomly on the field record with `wait-times` τ_a and τ_b

$$T_f(\tau) = a * \delta(t - \tau_a) + b * \delta(t - \tau_b). \tag{6}$$

Correlation in the Fourier domain by equation 3 yields

$$T_f T_f^* = AA^* + BB^* + AB^* \mathrm{e}^{-i\varpi(\tau_a - \tau_b)} + BA^* \mathrm{e}^{-i\varpi(\tau_b - \tau_a)} \,. \tag{7}$$

The sum of the first two terms is the result dictated by equation 1. The second two are extra. If $|\tau_b - \tau_a| > \max(t)$, one term will be purely acausal, and the other at very late lags that can be windowed away in the time domain. However, if the operation is performed in the Fourier domain, circular correlation is actually implemented and energy from the cross-terms may not so easily be avoided. If $|\tau_b - \tau_a| < \max(t)$, the cross-terms are included in the correlated gathers.

Redefine A and B as the impulse response of the earth, I_e, convolved with source functions, F which now contain their phase delays. As such, the cross-terms of equation 7 are

$$AB^* = (F_a I_e)(F_b I_e)^* = F_a F_b^* \, I_e^2 = F_c \, I_e^2 \,. \tag{8}$$

Like the first two terms in equation 7, the cross-terms have the desired information about the earth. However, the source function f_c included is not zero phase. These terms are the *other-terms* or virtual multiples in Schuster et al. (2004). If the source functions are random series, terms with residual phase (such as $F_c I_e^2$ above) within the gathers will decorrelate and diminish in strength as the length of f and the number of cross-terms increases. While we may hope to collect a large number of sources, it is probably unreasonable to expect many of them to be random series of great length.

The inclusion of these cross-terms in the correlation output produces a data volume

$$\tilde{R}(\mathbf{x}_r, \mathbf{x}_s, \varpi) \neq R(\mathbf{x}_r, \mathbf{x}_s, \omega) \,.$$

The ratio of desirable zero-phase terms to cross-terms containing residual phase decreases as $1/(n_s - 1)$. $\tilde{R}$ is not especially useful however. The inclusion of the cross-terms between the experiments returns a data volume that may not be more interpretable than the raw data. This

will be the case if the individual source functions are correlable or not conveniently located along the τ-axis such that all of their correlated phase terms, F_c in equation 8, are zero. These virtual multiple events will likely be more problematic than conventional multiples as every reflector can be repeated $n_s!/(n_s-2)!$ times.

Figure 2 shows the effect of the cross terms expanded in equation 8. The figure is directly analogous to Figure 1, though with two important differences. First, there are overlapping source function-reflection pairs. Second, the direct arrivals are spaced randomly along the time axis rather than engineering them to lie at the first sample of one of the short subsections. The second source arrives at the receiver before the reflection from the first source. The third source is randomly placed at the far end of the trace. The traces on the right are zoomed versions of their counterparts to the left. The result desired by a passive seismologist trying to produce a zero-offset trace from R, bottom trace Figure 1, can not be produced. The middle trace was correlated in the Fourier domain and transformed back to time. The bottom trace was computed by stacking eight windows from the input before correlation. The difference between the two output traces is not from reordering the summation for the Fourier transform in equation 5. Actually, this is the aliasing of the autocorrelation result itself. Both methods produce the wrong result at almost all times. They are however correct and identical at one location: zero-lag.

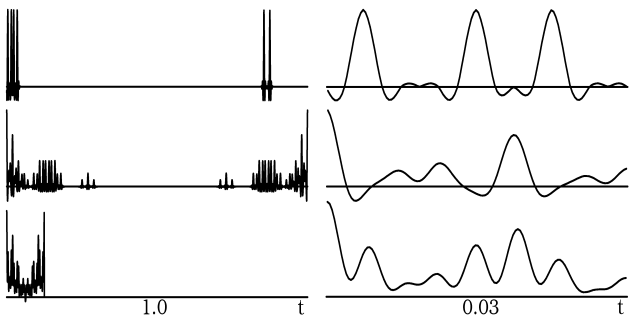

Figure 2: Right panel is 32x zoom of left. (top) Idealized signal of three identical subsurface sources. First two direct-reflection pairs overlap. (middle) Autocorrelation. (bottom) Autocorrelation performed after stacking 8 constituent windows. Zero values are padded on the bottom trace to facilitate plotting. brad1-freq2 [ER]

Figure 3 shows a more complicated example of the effective summation of source terms during the Fourier transform. The first two panels are individual transmission wavefields from sources at the left side of the model and just to the right of the center of the model. Notice that the wavefields have been carefully windowed to assure that the minimum traveltime for the two wavefields is the same. The model is a constant velocity medium with two diffractors in the center. The right panel is the sum of 225 similar sources covering the bottom of the velocity model. Summing the many shots has created a zero-offset data volume that could be migrated with a planewave migration algorithm. Cross-correlating this data to produce shot-gathers produces several dozen flat plane-waves and only the faintest hint of a ringing train of diffraction hyperbolas. $\tilde{R} \neq R$ due to processing T_f rather than the individual $T(\xi)$ records. Figure 4 mimics Figure 3 directly without having taken care to align the direct arrivals to the same time sample. The summation of all 225 wavefields gives the result on the right. Cross-correlating this data to produce shot-gathers makes a very messy plot.

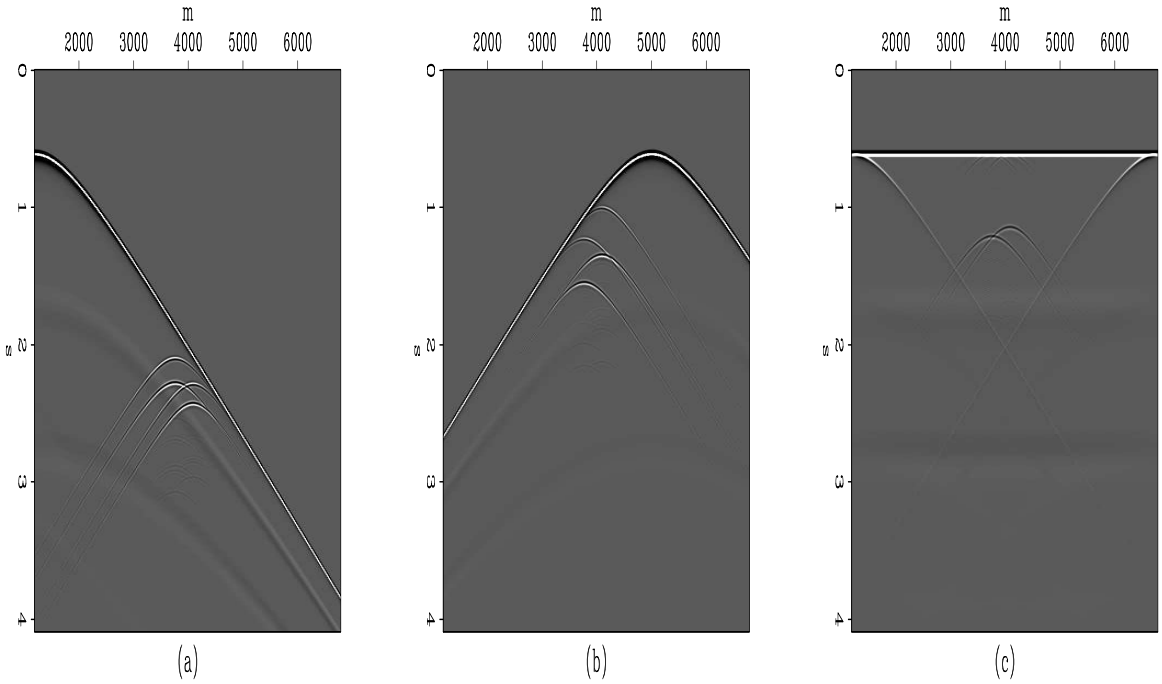

Figure 3: (a) Transmission wavefield from a subsurface source below $x = 1200m$ in a model containing two diffractors. (b) Transmission wavefield from source below $x = 5000m$. (c) Sum of 225 modeled wavefields. brad1-diff.noshift [CR]

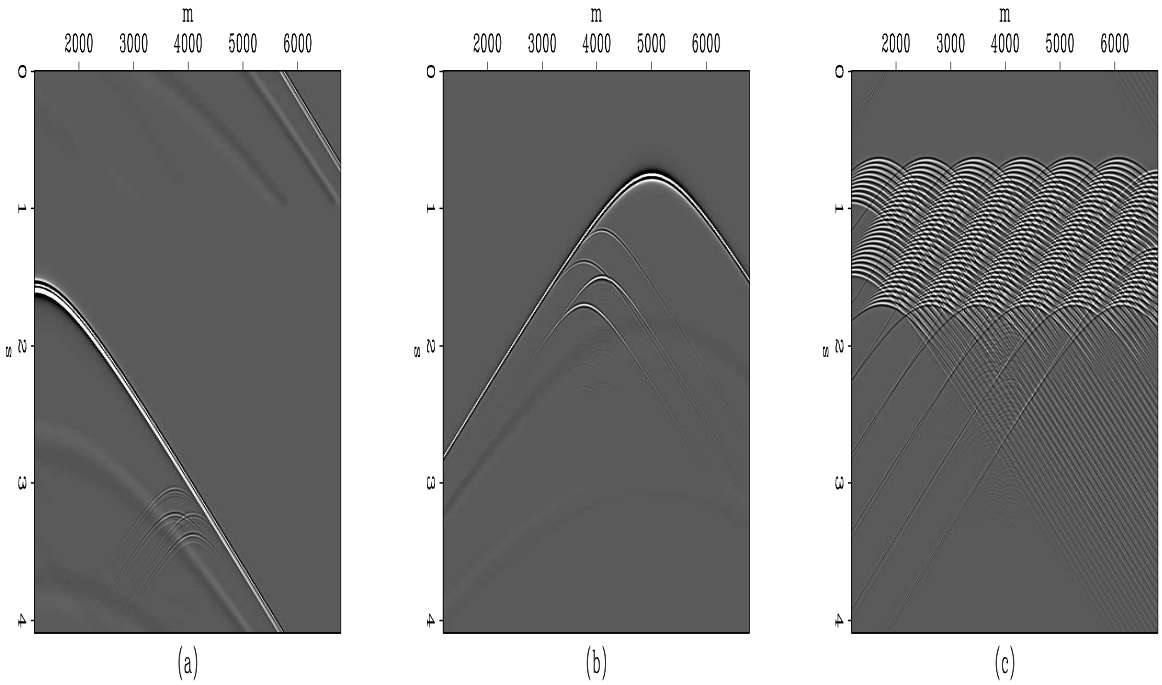

Figure 4: (a) Transmission wavefield from a source below $x = 1200m$ in a model containing two diffractors. (b) Transmission wavefield from source below $x = 5000m$. (c) Sum of all wavefields. brad1-diff.shift [CR]

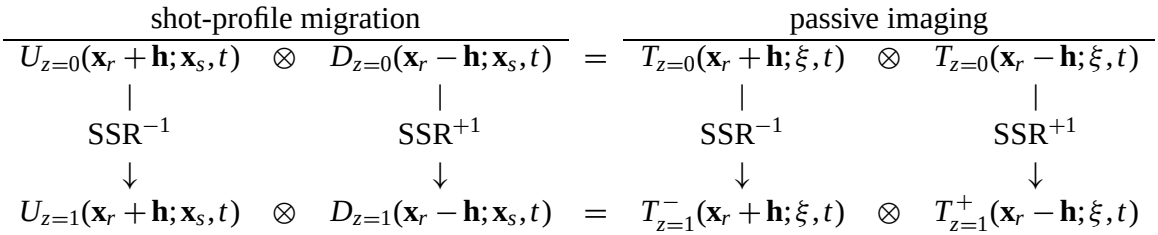

Figure 5: Equivalence of shot-profile migration of reflection data and direct migration of passive wavefields. $T(\xi,t)$ are the wavefields of equation 1. $\mathbf{x}_s$ has a similar meaning to ξ. Only first and second levels of the iterative process are depicted. $\sum_{\mathbf{x}_s}$ and $\sum_{\omega}$ produces the image $i_z(\mathbf{x}_r,\mathbf{h})$ for both methods.

DIRECT MIGRATION

The correlated wavefield $\tilde{R}$ is not usable by the majority of available reflection migration data tools. The source axis summation explained above does not remove all of the potential time delays. However, field data can still be migrated with a scheme that includes separate extrapolation and correlation (for imaging) steps. Artman and Shragge (2003) shows the applicability of direct migration for transmission wavefields with a shot-profile algorithm. Artman et al. (2004) provides the mathematical justification (for zero phase source functions). Simply stated, both Fourier domain extrapolation across a depth interval and correlation are diagonal square matrices, and thus commutable. This means that the correlation required to calculate the earth's reflection response from transmission wavefields can be performed after extrapolation with the shot-profile imaging condition (Rickett and Sava, 2002)

$$i_z(\mathbf{x},\mathbf{h}) = \delta_{\mathbf{x},\mathbf{x}_r} \sum_{\mathbf{x}_{s_k}} \sum_{\omega} U_z(\mathbf{x}_r+\mathbf{h};\mathbf{x}_{s_k},\omega) D^*_z(\mathbf{x}_r-\mathbf{h};\mathbf{x}_{s_k},\omega)\,, \tag{9}$$

where T is used for both upcoming, U, and downgoing, D, wavefields.

Figure pictorially demonstrates how direct migration of field passive seismic data fits into the framework of shot-profile migration to produce the 0^{th} and 1^{st} depth levels of the zero offset image. The sum over frequency has been omitted to reduce complexity in the figure. Also, after the first extrapolation step, with the two different phase-shift operators, the two transmission wavefields are no longer identical, and can be redefined U and D. This is noted with superscripts on the T wavefields at depth.

Shot-profile migration becomes planewave migration if conventional shot-gathers are summed for wavefield U, and a horizontal plane source is modeled for wavefield D. Partial summation of conventional shot-records will introduce cross-talk into the image. Only by summing enough shots so that their destructive interference cancels out their cross-talk can one produce a high quality image. For raw passive data, the sum over sources leads to an areal wave with complicated temporal topography. Moving the sum over shots in the imaging condition of equation 9 to operate on the wavefields rather than their correlation, changes shot-profile

$$
\begin{array}{ccccc}
\multicolumn{3}{c}{\text{planewave migration}} & & \text{passive wavefront imaging} \\
\left(\sum_{\mathbf{x}_s} U_{z=0}(\mathbf{x}_r+\mathbf{h};\mathbf{x}_s,t)\right) & \otimes & \left(\sum_{\mathbf{x}_s} D_{z=0}(\mathbf{x}_r-\mathbf{h};\mathbf{x}_s,t)\right) & = & T_{z=0}(\mathbf{x}_r+\mathbf{h},\tau) \otimes T_{z=0}(\mathbf{x}_r-\mathbf{h},\tau) \\
\downarrow & & \downarrow & & \downarrow \quad \downarrow \\
\text{SSR}^{-1} & & \text{SSR}^{+1} & & \text{SSR}^{-1} \quad \text{SSR}^{+1} \\
\downarrow & & \downarrow & & \downarrow \quad \downarrow \\
U_{z=1}(\mathbf{x}_r+\mathbf{h},t) & \otimes & D_{z=1}(\mathbf{x}_r-\mathbf{h},t) & = & T^{-}_{z=1}(\mathbf{x}_r+\mathbf{h},\tau) \otimes T^{+}_{z=1}(\mathbf{x}_r-\mathbf{h},\tau)
\end{array}
$$

Figure 6: Equivalence of direct migration with simultaneous migration all shots in a reflection survey. $T(\tau)$ is the field data wavefield of equation 3. Only first and second levels of the iterative process are depicted. $\sum_\omega$ produces the image $i_z(\mathbf{x}_r,\mathbf{h})$ for both methods.

migration to something akin to planewave migration which I will call wavefront migration.[2] Like planewave migration, after even a few wavefields have been combined, the best course of action is to sum all the sources to attain good areal coverage of the source wavefront to minimize cross-talk. Figure shows the change source summation has on both conventional shot migration and direct passive migration. Notice the parameterization of $T(\tau)$ meaning field data (where the depth subscript displaces the use of T_f). Importantly, the data input into the migration needs to have the late lags windowed before input into the migration as they have no correspondence to the subsurface structure. This can be accomplished by any of the three options discussed above: correlation followed by windowing, DFT followed by subsampling, or stack followed by DFT and correlation.

SYNTHETIC EXAMPLES

Data was also synthesized through a model containing two synclines. Figure 7a shows summed wavefields with the same direct arrival time. Panel (b) is the sum of the same wavefields after applying random phase delays to each. Panel (b) has all sources firing within the 4 seconds plotted, which results in some wrap-around. Bandlimited impulses were used as sources without any addition of randomness. Figure 8 shows zero offset images produced by direct migration of the data shown in Figure 7. Panel (b) is not as high quality as panel (a). A faint reflection mimicking the first event can be seen at $z = 350m$. This could be in part from events wrapping around the time axis when applying their respective phase delays. This is probably a worst-case result, that can be avoided by processing a time-window several times longer than the minimum, t. Given the dramatic departure of the data Figure 7b) from a horizontal planewave source, significant energy may also be at $\mathbf{h} \neq 0$. The most obvious difference is the diminution of the multiple from the first reflector at $z = 485$. The second reflector is much clearer in panel (b) without its interference.

[2]As such, the subsurface offset axis of the image will probably not be densely populated. To fill the offset axis, multiple planewave migrations can be summed after convolving the data with various ray parameters (Sun et al., 2001; Liu et al., 2002).

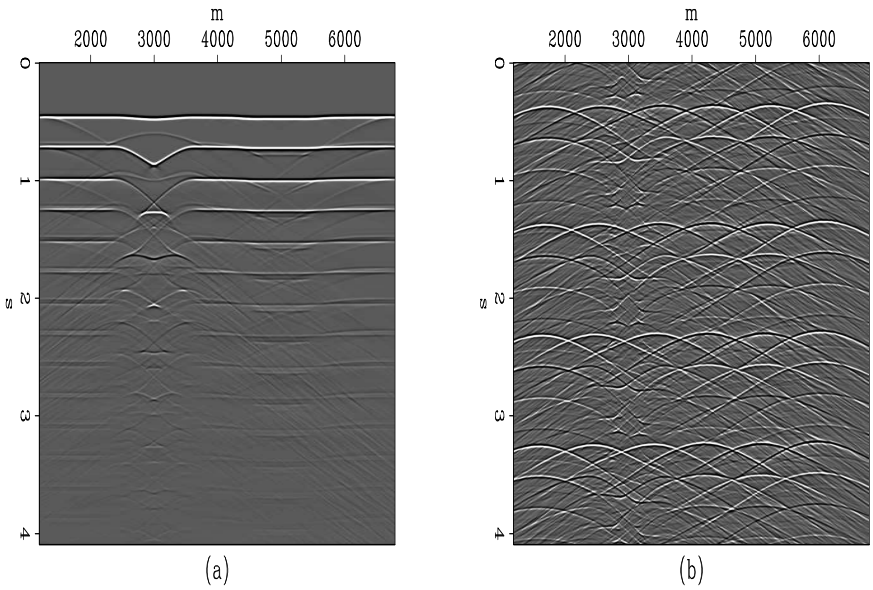

Figure 7: (a) Perfectly stacked shots from a double syncline model. (b) Stack of wavefields after applying a random time delay in the Fourier domain. brad1-dat.syn [CR]

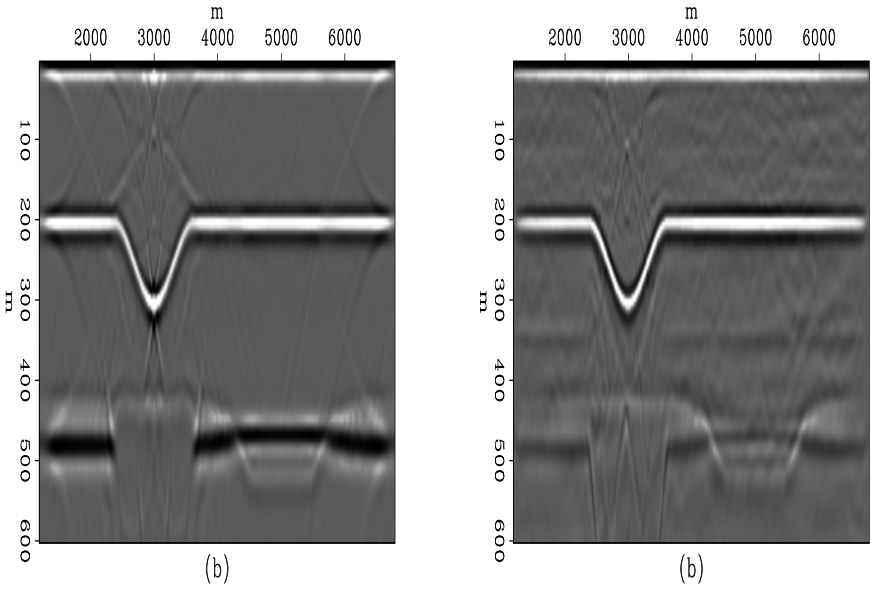

Figure 8: (a) $\mathbf{h} = 0$ image produced by direct migration of Figure 7 panel (a). (b) $\mathbf{h} = 0$ image produced by direct migration of Figure 7 panel (b). brad1-mig.syn.norand [CR]

CONCLUSION

Processing windowed subsets of a passive survey may be advantageous. If time-localized events are present, such as teleseismic arrivals, one can process smaller time windows when sure of significant contribution to the image. Without knowing of if or how many sources are active within the bulk of the data, long correlations of the raw data are an almost inevitable approximation (equation 3) to the rigorous definition for synthesizing shot-gathers from transmission wavefields (equation 1). Accepting this reality, first aliasing the time data reduces the computation cost for a DFT by $1/n_\tau$ (where n_τ is the number of samples in the long input trace)[3] without any further approximation. Rather, it simply capitalizes on the original approximation without having to assume uncorrelable white source functions.

The inherent aliasing within the approximation sums the source functions within the output. This superposition of sources does not produce $R(\mathbf{x}_r, \mathbf{x}_s, \omega)$ under realistic situations. Instead the result is, $\sum_{\mathbf{x}_s} R(\mathbf{x}_r, \mathbf{x}_s, \varpi)$. This data volume can only be migrated with an algorithm that can accept generalized source functions (parameterized by space and time), and uses a correlation imaging condition. Both of these conditions are enjoyed by shot-profile migration.

Migrating all sources at the same time removes the redundant information from a reflector as a function of incidence angle. This makes velocity updating after migration impossible. At this early stage, I contend that passive surveys will only be conducted in actively studied regions where very good velocity models are already available. If this becomes a severe limit, the incorporation of planewave migration strategies can fill the offset dimension of the image.

In practice, the length of the aliased windows should probably be several times longer than the minimum time to the deepest reflector. Multiple sources within this time are handled perfectly by direct migration, and the risk of adding the end of the reflection series to the beginning of the record will be minimized. The decision can be determined by whatever compute resources are available for the size of the data set collected. However, if the time support of the wavefield migrated is many times longer than appropriate for the deepest reflector of interest, aphysical correlation lags will introduce coherent noise into the image that will look exactly like reflections.

REFERENCES

Artman, B., and Shragge, J., 2003, Passive seismic imaging: AGU Fall Meeting, Eos Transactions of the American Geophysical Union, Abstract S11E–0334.

Artman, B., Draganov, D., Wapenaar, C., and Biondi, B., 2004, Direct migration of passive seismic data: 66th Conferance and Exhibition, EAGE, Extended abstracts, P075.

Liu, F., Stolt, R., Hanson, D., and Day, R., 2002, Plane wave source composition: An accurate phase encoding scheme for prestack migration: Soc. of Expl. Geophys., 72nd Ann. Internat. Mtg, 1156–1159.

[3] n_τ will be $O(10^7)$ for just one day of data collected at 0.004s sampling rate.

Nowack, R. L., Dasgupta, S., Schuster, G. T., and Sheng, J., 2003, Correlation migration of scattered teleseismic body waves with application to the 1993 cascadia experiment:, *in* Fall Meet. Suppl. Abstract S32A-0835.

Rickett, J. E., and Sava, P. C., 2002, Offset and angle-domain common image-point gathers for shot-profile migration: Geophysics, **67**, no. 03, 883–889.

Schuster, G., Yu, J., Sheng, J., and Rickett, J., 2004, Interferometric/daylight seismic imaging: Geophysics Journal International, **157**, 838–852.

Sun, P., Zhang, S., and Zhao, J., 2001, An improved plane wave prestack depth migration method: Soc. of Expl. Geophys., 71st Ann. Internat. Mtg, 1005–1008.

Wapenaar, K., Thorbecke, J., and Draganov, D., 2004, Relations between reflection and transmission responses of three-dimensional inhomogeneous media: Geophysical Journal International, **156**, 179–194.

Yu, J., and Schuster, G., 2004, Enhancing illumination coverage of vsp data by cross-correlogram migration:, *in* 74th Ann. Internat. Mtg. Soc. of Expl. Geophys., 2501–2504.